

Volume Bragg Grating improves characteristics of resonantly diode pumped Er:YAG 1.65- μm DPSSL

Igor Kudryashov ^{a)} and Dmitri Garbuzov

Princeton Lightwave Inc., 2555 US Route 130, Cranbury, New Jersey, 08512

Mark Dubinskii

U.S. Army Research Laboratory, AMSRD-ARL-SE-EO, 2800 Powder Mill Road, Adelphi, Maryland 20783

ABSTRACT

Significant performance improvement of the Er(0.5%):YAG diode pumped solid state laser (DPSSL) has been achieved by pump diode spectral narrowing via implementation of external volumetric Bragg grating (VBG). Without spectral narrowing, with a pump path length of 15 mm, only 37% of 1532 nm pump was absorbed. After the VBG spectral narrowing, the absorption of the pumping radiation increased to 62%. As a result, the incident power threshold was reduced by a factor of 2.5; the efficiency increased by a factor of 1.7, resulting in a slope efficiency of ~23%. A maximum of 51 W of CW power was obtained versus 31 W without the pump spectrum narrowing.

Keywords: Er:YAG , diode-pumped; volumetric Bragg grating; solid-state lasers.

1. Introduction

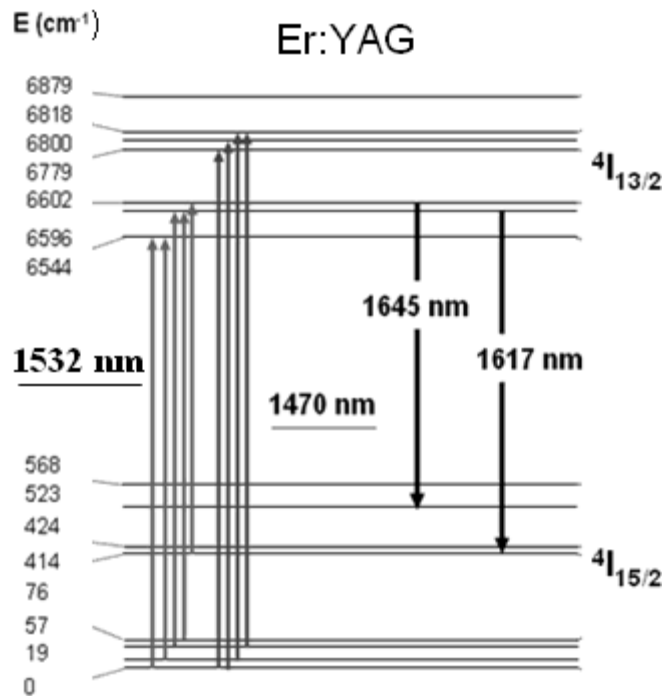


Fig. 1. Er³⁺:YAG energy levels along with absorption and emission transitions in the 1.45-1.66 μm spectral range.

resonantly-pumped Er:YAG SSL with Er-fiber-laser as well as direct diode pumping [3-5]. Due to the dramatic strides

Growing interest to high power lasers in the eye-safe spectral domain initiated a new wave of activity in developing solid-state lasers based on Er³⁺-doped materials. Er³⁺:YAG has good mechanical, thermal and thermo-optic properties and is one of the most attractive active materials for developing ~1.6- μm eye-safe SSL. Most importantly, it has resonantly-pumped operation mode very similar, and in some ways better than, Yb:YAG laser. Spectroscopy of 1450 \leftrightarrow 1660-nm transitions between the 4I_{13/2} and 4I_{15/2} Stark-split manifolds in Er³⁺:YAG, forming a quasi-three level system (Fig.1), has been studied by numerous scientific groups (e.g., [1,2]). Four upper states of the eight Stark components of the ground 4I_{15/2} manifold serve as the terminal states for Er³⁺ laser transitions with the wavelengths ranging from 1617 to 1660 nm. Compared to co-dopant assisted excitation used for pumping Yb:Er:YAG-based SSL, major advantage of the Er:YAG resonant pumping into 1470 and 1532 nm bands is low quantum defect. It allows for shifting significant part of thermal load from Er-doped gain medium itself to the pump diodes, thus greatly reducing gain medium thermal distortions deleterious to SSL power scaling with high beam quality. Recently significant progress has been made in development of

^{a)} E-mail: ikoudriachov@princetonlightwave.com

in the Quantum Well Separate Confinement Heterostructure (QW SCH) lasers based on InGaAsP/InP systems [6,7], direct diode pumping delivers impressive efficiency results which are highly competitive with those received with Er-fiber laser pumping. Majority of problems with pumping Er:YAG by InP laser diodes are associated with pumping spectral width being much wider than spectral width of GaAs-based laser diodes used for Yb,Er:YAG pumping. Optimization of InP laser diode design [7] allowed to reduce the pump output full width at half maximum (FWHM) to 7-8nm, but it is still too wide to match individual Er:YAG absorption lines. One of the most promising approaches to proper InP diode spectral narrowing consists in using the volumetric Bragg grating (VBG) as highly efficient selective feedback element [8]. Reported here is significant performance improvement of the Er(0.5%):YAG DPSSL, which was achieved by pump diode spectral narrowing via implementation of external Bragg grating. 51 W of CW Er:YAG power was achieved versus 31 W without the pump spectrum narrowing.

2. Experiment

A 0.5% Er:YAG slab was used in our experiments. Low doping level was chosen to minimize Er^{3+} upconversion losses [9]. Laser slab sized 10x15x2.5 mm was In-bonded to water cooled copper heatsink. All measurements were done with the cooling water temperature $\sim 15^\circ\text{C}$. The two 2.5 x 10 mm sides were polished and had antireflective coatings ($R < 0.2\%$) at 1645 nm. 1530-nm stack of ten 1-cm laser diode arrays mounted on microchannel coolers (pitch 1.8 mm) was used for pumping. Each array was fast axis and slow axis collimated (FAC and SAC). Schematic diode pumped Er^{3+} :YAG laser setup is shown in Fig. 2. Fig.2a demonstrates pump ray-tracing results in the slab plane. Fig.2b and Fig.2c (detailed slab view) demonstrate pump ray-tracing results in the plane perpendicular to the slab. Two cylindrical lenses with focal lengths of 100 and 30 mm were used to launch pumping into the slab through the dichroic mirror M1. Laser cavity comprised two flat mirrors M1 ($>99.8\%$ @1645nm) and M2 (output coupler), total cavity length was 50 mm. Output couplers with reflectivities of 98%, 96%, 93% and 85% were used in order to optimize laser performance. DPSSL was tested with and without diode spectral narrowing by VBG. VBG sized at 23x14x1.5mm, nominal reflectivity 20% , was supplied by Ondax, Inc. Nominal central wavelength was 1531.5 nm. Heated air flow was used for wavelength fine tuning and stabilization around 1532.5 nm.

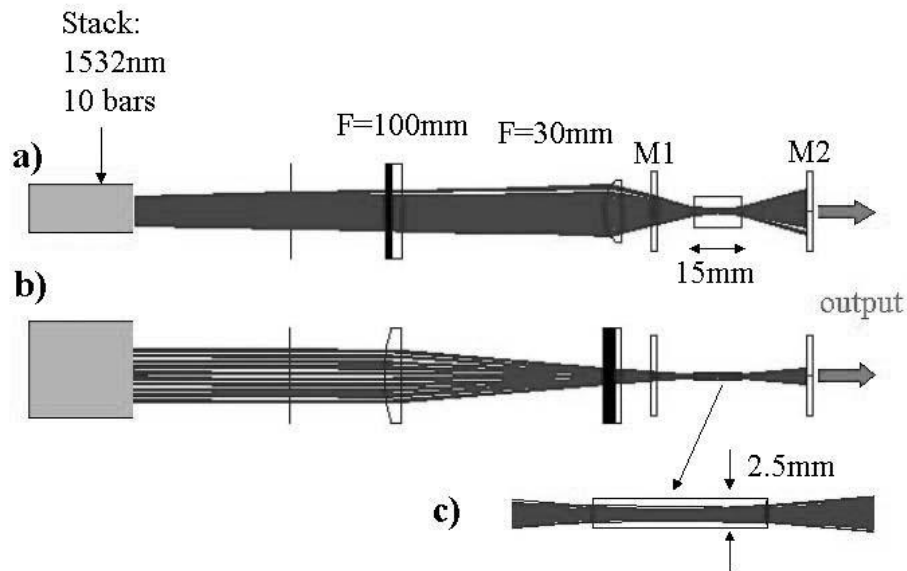


Fig. 2. Schematic view of SSL: a) pump ray-tracing in the slab plane; b) pump ray-tracing in the plane perpendicular to the slab; c) detailed view of pump ray-tracing in the plane perpendicular to the slab

3. Results and discussion

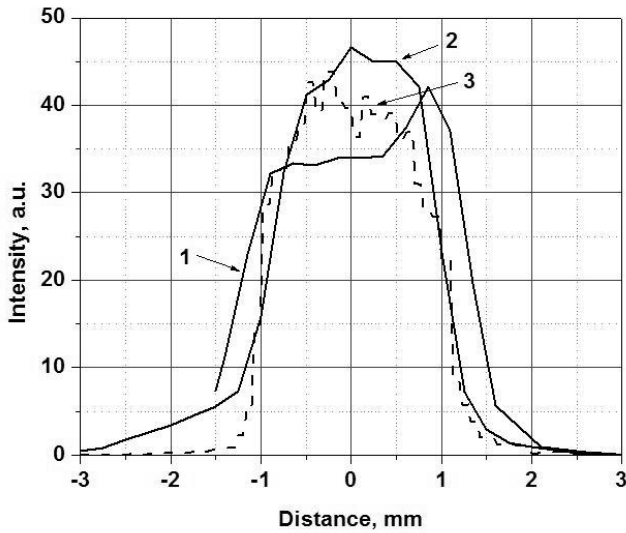


Fig. 3 Pump spot in the slab plane: 1- power distribution at the front face of the slab, 2 – power distribution (in air) at 9 mm from the front face, 3 – calculated spot on the back face

The pump incident power and spectra were measured after the dichroic mirror M1 (Fig. 2) to eliminate ambiguities associated with the spectral complexity of the coating. Measured in this location typical spectrum from the stack without VBG is shown in Fig. 4 (plot 1). As can be seen, the spectral FWHM of the pump is about 9 nm and is much wider than the width of the individual absorption line. Multiple (and overlapping!) absorption lines - a “band” - around 1532 nm do help increasing the absorbed fraction of the incident power, but from the spectrum taken after the Er³⁺:YAG slab (plot 2) one can see that significant fraction of pump power does not get absorbed.

The VBG-narrowed InGaAsP/InP stack spectra taken before and after the Er³⁺:YAG slab are shown in Fig. 5. The spectra in Fig. 4 and Fig. 5 were measured for the same stack temperature and current through the stack. It can be seen that spectrally-selective feedback from VBG leads to significant redistribution of the spectral power density from the stack without significant reduction of the stack power.

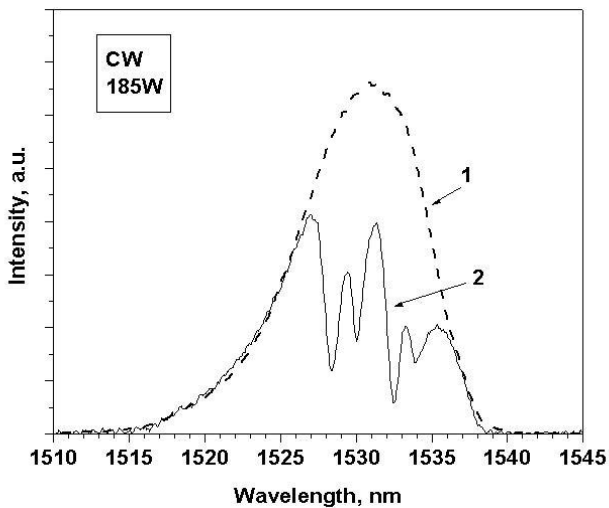


Fig. 4. Pump spectra before (1) and after the slab (2) for the InGaAsP/InP stack without VBG

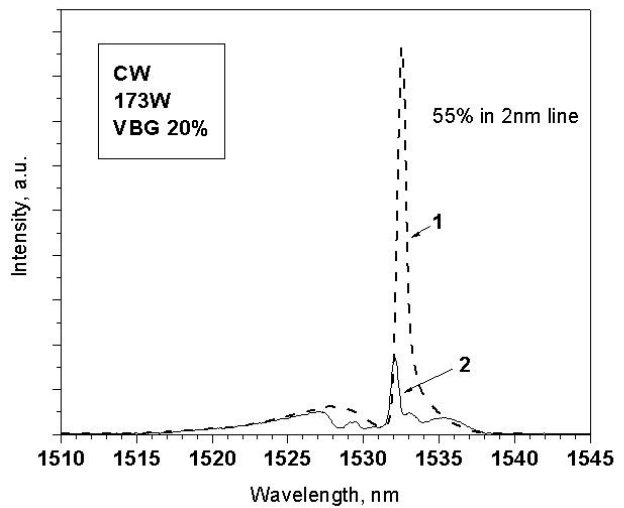


Fig. 5. Pump spectra before (1) and after the slab (2) for the VBG-narrowed InGaAsP/InP stack

The cross-section of the pump beam in the crystal was measured to define the actual dimensions of the gain region. The results for the beam intensity distribution in the slab plane are shown in Fig. 3. Measurements were carried out in air, but, taking into account the ~1.8 refractive index of YAG, we assumed that the beam cross-section measured ~9 mm from the slab front (pump) face corresponds to the actual beam cross-section on the back face. Plot 1 indicates power distribution at the front face of the slab. Plot 2 - measured power distribution on the back face. Plot 3 is the simulated (by optical design program ZEMAX) beam cross-section on the back face of the Er³⁺:YAG slab (5mrad x 40mrad divergences for individual arrays were used as simulation parameters). One can see that the distribution measured in the back plane of the laser crystal fully confirms the validity of our ZEMAX simulation.

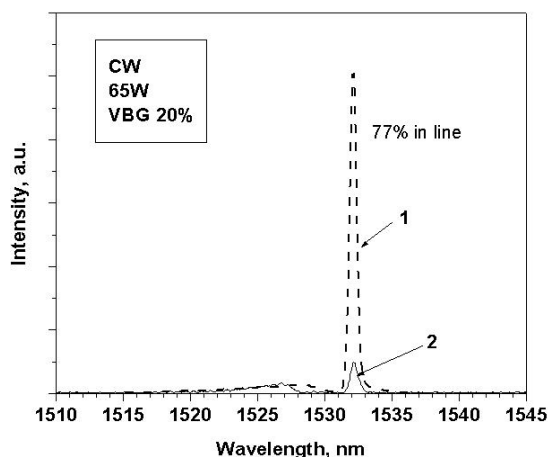


Fig. 6. Pump spectra before (1) and after the slab (2) for the VBG-narrowed InGaAsP/InP stack - at low power

choice of a proper effective VBG reflectivity is a trade off between the required efficient line-narrowing and loss of stack power caused by VBG reflection. In our case, at 20% VBG reflectivity, the reduction in total stack power upon spectral narrowing at ~180 W power level did not exceed 6.5%.

The VBG spectrum stabilization and narrowing will significantly affect the absorbed fraction of pump power in the slab. It is clearly demonstrated in Fig. 7. Plot 1 shows the absorbed fraction of pump power versus incident pump power for the VBG stabilized stack. Plot 2 illustrated the similar dependence for stack without the VBG. Plots 3 (and the scale on the right) indicate the ratio between the points from plots 1 and 2. All these dependences were measured without the mirror M2 (Fig.2), i.e., they correctly reflect the gain medium behavior before the threshold. It is clear that the absorbed fraction of pump power after the threshold will remain constant (assuming there is no severe thermal effects). Top scale shows the incident power density calculated from the estimated pumped volume of 0.056cm^3 . Stable position of the stack spectrum was controlled by water temperature through the stack in the entire range of the pump current, so that with increased stack output power only pump spectral widening took place.

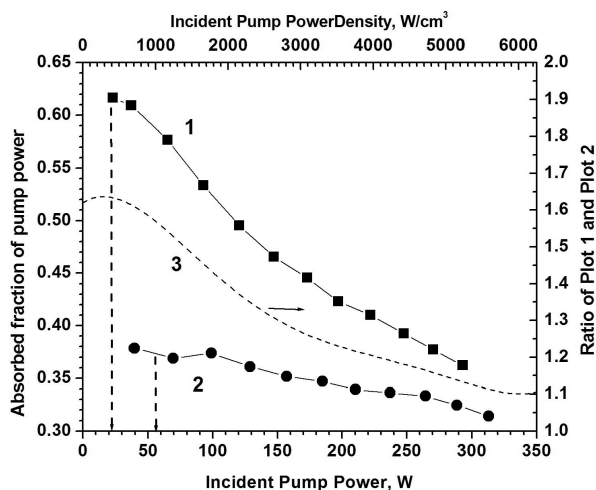


Fig. 7. Absorbed fraction of pump power for VBG-narrowed InGaAsP/InP stack (plot 1) and without VBG (plot 2) versus incident pump power (bottom scale) and incident pump power density (top scale). Right scale displays the ratio of plot 1 and plot 2.

At 173 W of total stack power about 55% is contained in the ~2-nm line, which dramatically increases the fraction of the pump absorbed by Er^{3+} :YAG slab. Fig. 6 displays the VBG-narrowed InGaAsP/InP stack spectra similarly taken before and after the Er^{3+} :YAG slab at significantly lower stack current and, hence, output power. At 65 W (as opposed to ~173 W in Fig. 5) the fraction of total power contained in the line increases up to 77%. In this case the fraction of the pump absorbed by Er^{3+} :YAG slab will go even higher – with respect to that shown in Fig. 5. Lower fraction of the total pump power contained in the line in Fig. 5 can be explained by a combination of the weak feedback from VBG (seen by stack) and the trend of spectral widening at higher currents through the InGaAsP/InP stack. VBG feedback is weak because the coupling efficiency of the VBG-reflected light into individual emitters of the stack is much lower than 100%. The

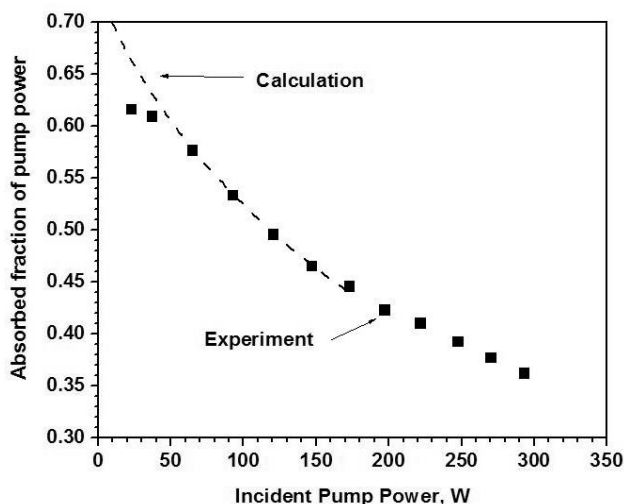


Fig. 8. Comparison of calculated absorbed fraction of pump power in 1532.5nm line and experimental data obtained for VBG-stabilized stack versus incident power

As seen from Fig. 7 the absorbed fraction of pump power for the VBG stabilized pump source is always higher than that for the source without the VBG stabilization. In the low incident power range the absorbed fraction is 1.6 times higher for the VBG-stabilized pump source. But VBG-stabilized pump power no longer offers such a significant advantage at much higher incident pump power. There are two reasons for that. First, as mentioned before, the pump source spectrum is wider at higher power levels and stabilization/narrowing effect of VBG becomes less efficient (as is also seen from Fig. 5 and Fig. 6). Surely, reduction of the power fraction in a ~2nm-wide line is partially compensated by absorption in the adjacent absorption lines. The second factor, which reduces the absorption at high incident power, is caused by ground-state depletion effect (bleaching). Based on the theory by R. Beach [10], we calculated the absorption versus incident power (for “ideally-stable” 1532.5nm pump source) in order to estimate the contribution of bleaching in the above experimental results. The threshold incident power according to [10] is:

$$P_{th} = \frac{h\nu_p N_2 V}{\eta_{del} \tau (1 - e^{-\sigma_p N_{2p} L})} \quad (1)$$

where: h is Planck’s constant, ν_p - pump transition frequency, η_{del} - pump delivery efficiency (assumed to be 1.0 in our case), N_2 - excited state manifold density at threshold, V - active media volume, τ - excited manifold storage lifetime (with taken into account upconversion rate), σ_p - spectroscopic cross section for the pump radiation, N_{2p} - density coupled by pump radiation, L - absorption length.

The absorbed fraction of pump power in this case is:

$$A = 1 - e^{-\sigma_p N_{2p} L} \quad (2)$$

Comparison of the calculated absorbed fraction of pump power in 1532.5nm line and experimental data obtained for VBG-stabilized stack versus incident power is shown in Fig. 8. This comparison allows concluding that the bleaching effect clearly dominates in our experimental conditions. So, in order to fully utilize the advantages of pump spectral

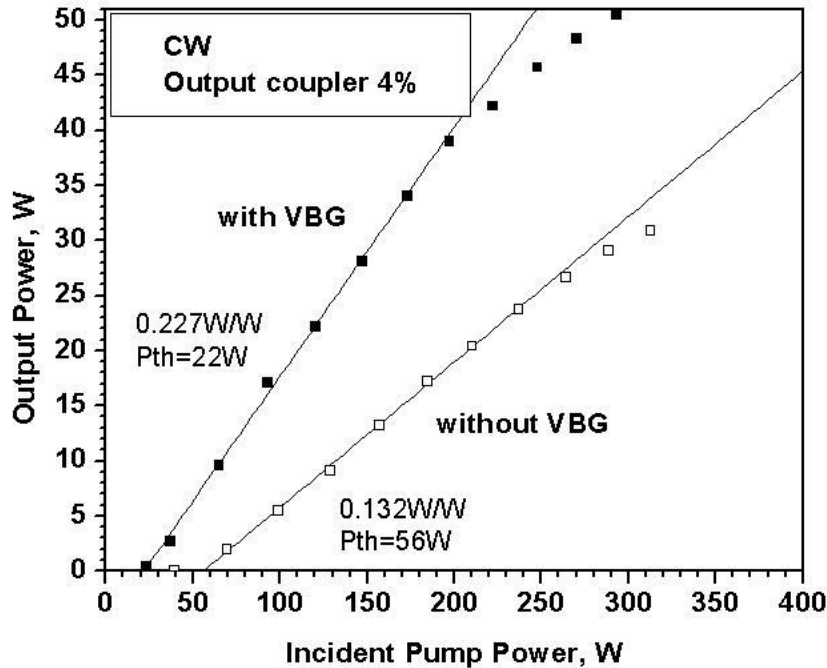


Fig.9. Er³⁺:YAG DPSSL output power versus incident pump power for VBG stabilized pump source (solid squares) and pump source without VBG (hollow squares). Output coupler: T=4%

narrowing by VBG it is important to work in the low threshold power density range. The cumulative effect of pump spectrum stabilization and narrowing on the performance of resonantly-pumped Er^{3+} :YAG DPSSL is demonstrated in Fig. 9. The CW output power of Er^{3+} :YAG DPSSL versus incident pump power for the VBG-stabilized pump source (solid squares) and pump source without VBG (hollow squares) are measured at 4% output coupler. Comparison in Fig. 9 demonstrates significant improvement of the Er^{3+} :YAG DPSSL performance by spectrally narrowing the pump. Slope efficiency increased 1.7 times and threshold power decreased 2.5 times. Output power is doubled in the range of incident pump powers up to 200W. Linearity of the output power versus incident pump power dependence in this range corroborates our assumption that reduction of the absorbed fraction of pump power at higher incident pump powers is caused by the bleaching effect. In a range of incident powers beyond 200W the use of VBG-stabilized InGaAsP/InP stack is less advantageous due to thermal effects in the slab and increasing pump source effective spectral width. The maximum output power achieved in our experiments was 51W and 31W for Er^{3+} :YAG DPSSL with the VBG-narrowed InGaAsP/InP pump and the pump without VBG, respectively.

Fig. 10 shows the Er^{3+} :YAG DPSSL output power versus incident pump power for a set of different output couplers: T=2% (solid squares), T=4% (solid circles), T=7% (solid upward triangles) and 15% (solid downward triangles). It is clear that the optimum outcoupling loss resides in the range of 4-7%. This is best illustrated in Fig. 11, which indicates the absorbed threshold power and slope efficiency (per absorbed power) versus output coupler loss (%). In the 4% to 7% outcoupling loss range slope efficiency has a relatively narrow plateau wherein the threshold power does not increase enough to degrade of SSL performance. The slope efficiency in that range is about 0.37-0.38 per absorbed power (it corresponds to about 40% photon to photon efficiency). We had relatively limited set of output couplers in order to do the comprehensive analysis of internal losses and pumping efficiency to better understand efficiency limiting factors.

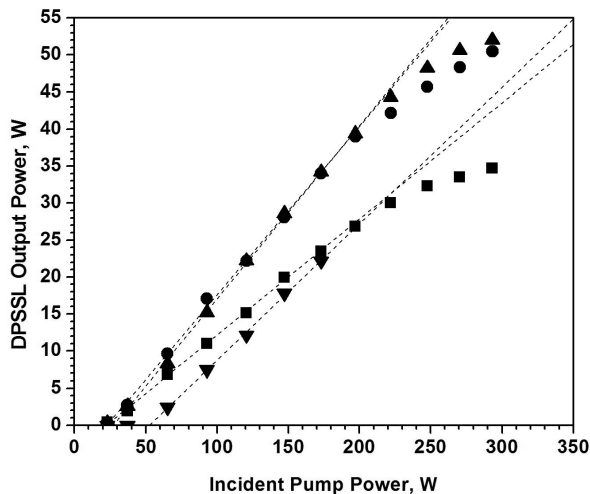


Fig. 10. Er^{3+} :YAG DPSSL output power versus incident pump power at output coupler T=2% (solid squares), T=4% (solid circles), T=7% (upward solid triangles), T=15% (downward solid triangles) for the VBG-narrowed pump

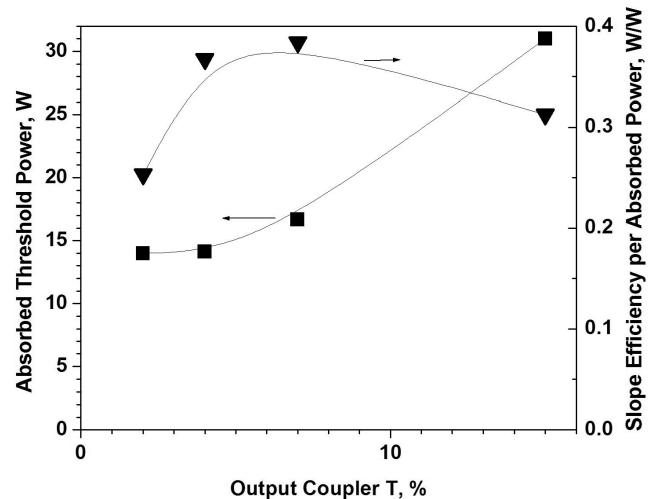


Fig.11. Absorbed threshold power (solid squares) and slope efficiency (solid downward triangles) per absorbed power versus output coupler transmission

4. Conclusion.

We reported significant CW performance improvement of the resonantly pumped Er :YAG solid state laser at 1.645- μm with direct pumping by a 1530-nm InGaAsP/InP FAC/SAC diode bar stack. This improvement has been achieved solely by implementation of VBG stabilization and spectral narrowing of the bar stack spectrum. Thus incident Er :YAG CW threshold power has been reduced by a factor of 2.5, the optical efficiency increased by a factor of 1.7, resulting in a slope efficiency of ~23% per incident power. We demonstrated the importance of keeping the laser in the low threshold power density range in order to be able to take full advantage of VBG stabilization. In the optimum range of output coupling loss (4-7%) absorbed threshold power was 14-17W and slope efficiency ~0.37-0.38 per absorbed

pump power. We obtained over 51 W of CW power in our experiments, which is, to the best of our knowledge, the highest CW power ever obtained from the resonantly-pumped Er:YAG laser with direct diode pumping.

This work was partially supported by the HEL-JTO/AF through the BAA Contract No.: FA9451-04-C-0189

5. References

1. N. Agladze, M. Popova, E. Vinogradov, T. Murina, V. Zhekov, "Oscillator Strength in $Y_3Al_5O_{12}-Er^{+3}$," *Opt. Commun.* **65**, p 351, (1988).
2. T. Schweizer, T Jensen, E. Heumann, G. Huber, "Spectroscopic Properties of Yb: Er:YAG," *Opt. Commun.* **118**, p. 557, (1995).
3. S. D. Setzler, M. P. Francis, Y. E. Young, J. R. Konves, and E. P. Chicklis, "Resonantly pumped eyesafe erbium lasers," *IEEE Journal of Selected Topics in Quantum Electronics* **11**, 645-657 (2005).
4. D. Hogenboom, M. Nguyen, H. Chou, "Good Beam Quality From a Diamond-cooled Er:YAG laser," *Proc. of SPIE* **6216**, (2006)
5. D. Garbuzov, I. Kudryashov, M. Dubinskii, "110W (0.9J) pulsed power from resonantly diode-laser-pumped 1.6- μ m Er:YAG laser", *Appl. Phys. Lett.* **87**, 121101 (2005)
6. P. Crump, T. Crum, M. DeVito, J. Farmer, M. Grimshaw, Z. Huang, S. Igl, J. Wang, W. Dong, "High Power 1470 nm Laser Bars and Stacks," *Technical Digest of SSDLTR 2004, Direct Energy Professional Society, Diode-3*.
7. D. Garbuzov, I. Kudryashov, A. Komissarov, "InGaAsP/InP Diode Laser Pumping Sources for Eye-Safe Solid-State and Fiber Lasers," *Optics East Conference*, paper 5594-37, (2004).
8. G. Venus, V. Smirnov, L. Glebov, and M. Kanskar, "Spectral Stabilization of Laser Diodes by External Bragg Resonator", *17th Annual Solid State and Diode Laser Technology Review, SSDLTR-2004 Technical Digest, Albuquerque, June 2004*.
9. M. Iskandarov, A. Nikitichev, A. Stepanov, "Quasi-two-level Er:YAG laser for 1.6 μ m range," *J. Opt. Technol.*, **68** (12), p. 885 (2001).
10. R.J. Beach, "CW theory of quasi-three level end-pumped laser oscillators", *Opt. Commun.* **123**, 385-393, (1995)